

Functional Interaction of Phospholipid Hydroperoxide Glutathione Peroxidase with Sperm Mitochondrion-associated Cysteine-rich Protein Discloses the Adjacent Cysteine Motif as a New Substrate of the Selenoperoxidase*

Received for publication, June 1, 2005, and in revised form, July 29, 2005. Published, JBC Papers in Press, September 13, 2005, DOI 10.1074/jbc.M505983200

Matilde Maiorino[‡], Antonella Roveri[‡], Louise Benazzi[§], Valentina Bosello[‡], Pierluigi Mauri[§], Stefano Toppo[‡], Silvio C. E. Tosatto^{¶1}, and Fulvio Ursini^{‡2}

From the [‡]Department of Biological Chemistry and [¶]Department of Biology and CRIBI Biotechnology Centre, Viale G. Colombo 3, University of Padova, I-35121 Padova and the [§]Institute for Biomedical Technologies, National Research Council, Viale Fratelli Cervi 93, I-2090 Segrate (Milano), Italy

The mitochondrial capsule is a selenium- and disulfide-rich structure enclashing the outer mitochondrial membrane of mammalian spermatozoa. Among the proteins solubilized from the sperm mitochondrial capsule, we confirmed, by using a proteomic approach, the presence of phospholipid hydroperoxide glutathione peroxidase (PHGPx) as a major component, and we also identified the sperm mitochondrion-associated cysteine-rich protein (SMCP) and fragments/aggregates of specific keratins that previously escaped detection (Ursini, F., Heim, S., Kiess, M., Maiorino, M., Roveri, A., Wissing, J., and Flohé, L. (1999) *Science* 285, 1393–1396). The evidence for a functional association between PHGPx, SMCP, and keratins is further supported by the identification of a sequence motif of regularly spaced Cys-Cys doublets common to SMCP and high sulfur keratin-associated proteins, involved in bundling hair shaft keratin by disulfide cross-linking. Following the oxidative polymerization of mitochondrial capsule proteins, catalyzed by PHGPx, two-dimensional redox electrophoresis analysis showed homo- and heteropolymers of SMCP and PHGPx, together with other minor components. Adjacent cysteine residues in SMCP peptides are oxidized to cystine by PHGPx. This unusual disulfide is known to drive, by reshuffling oxidative protein folding. On this basis we propose that oxidative polymerization of the mitochondrial capsule is primed by the formation of cystine on SMCP, followed by reshuffling. Occurrence of reshuffling is further supported by the calculated thermodynamic gain of the process. This study suggests a new mechanism where selenium catalysis drives the cross-linking of structural elements of the cytoskeleton via the oxidation of a keratin-associated protein.

More than 3 decades ago, evidence that radioactive selenium is concentrated in rat sperm mid-piece (1) and that severe selenium deficiency leads to male infertility (2) brought into focus the crucial role of this oligo-element in spermatogenesis. The pioneering studies of Calvin (3) and Pallini and Bacci (4) show that selenium bound to a 15–21-kDa

disulfide cross-linked protein is involved in the stabilization of the outer mitochondrial membrane of mammalian sperm. The protein was identified as a major component of the keratinous external layer of sperm mitochondrion, the so-called mitochondrial capsule (MC)³ in rat (5) and in bull (4), further confirming the structural role of selenium in spermatozoa (6). The electrophoretic overlapping of a cysteine-rich protein of the MC and radioactivity after *in vivo* ⁷⁵Se labeling supported the identification of the cysteine-rich protein as a selenoprotein (4, 6). The protein was therefore first named “MC protein” and then “MC selenoprotein” when Karimpour *et al.* (7), after the discovery that the co-translational selenocysteine insertion into protein requires an in-frame UGA codon (8), described three in-frame UGA codons at the 5' end of some mouse cDNA clones of the MC protein. It was later found that the open reading frame for the human protein does not contain any UGA codons, although the deduced protein shows a striking homology with the mouse protein, lying in repeated adjacent cysteine motif (9). It was eventually clarified that the mouse protein as well does not contain any selenocysteine and that the previously described three UGAs are actually located in the 5'-untranslated region of the mRNA. The MC protein was then renamed “sperm mitochondrion-associated cysteine-rich protein” (SMCP) (10). SMCP is expressed as a single gene product, mainly in the round spermatids of the testis seminiferous tubules (11). The rat protein sequence contains 12 Cys-Cys doublets and an additional 10 single Cys residues.

The issue of selenium content in the MC of spermatozoa was later clarified when a substantial amount of the selenoenzyme phospholipid hydroperoxide glutathione peroxidase (PHGPx; EC 1.11.1.12) was detected, in a cross-linked form, in rat sperm MC (12).

PHGPx is an active peroxidase in spermatids, and it becomes cross-linked and catalytically inactive in sperm MC. A thorough reduction of MC rescues active PHGPx, which catalyzes *in vitro*, in the presence of H₂O₂, the formation of aggregates, including all the MC proteins (12, 13). Among these, the polymerization of PHGPx has been positively detected (14). It takes place through the formation of a bond between selenium at the active site and cys 148 on the surface of the enzyme. This seleno-disulfide bond is formed when the limited availability of reducing substrate prevents the completion of the catalytic cycle, and thus represents a dead end of the reaction. This “suicidal” activity of PHGPx,

* This work was supported by the Italian Ministry of University and Scientific Research Grants PRIN 2003038920_002 (to M. M.) and 2004054995_001 (to F. U.). The costs of publication of this article were defrayed in part by the payment of page charges. This article must therefore be hereby marked “advertisement” in accordance with 18 U.S.C. Section 1734 solely to indicate this fact.

¹ Funded by a “Rientro dei cervelli” grant from the Italian Ministry of Education, and Research (MIUR).

² To whom correspondence should be addressed: Dept. of Biological Chemistry, Viale G. Colombo, 3, I-35121 Padova, Italy. Tel.: 39-049-8276104; Fax: 39-049-8073310; E-mail: fulvio.ursini@unipd.it.

³ The abbreviations used are: MC, mitochondrial capsule; KAPs, keratin-associated proteins; MS, mass spectrometry; PHGPx, phospholipid hydroperoxide glutathione peroxidase; RSCP, reduced-solubilized capsule proteins; SMCP, sperm mitochondrion-associated cysteine-rich protein; VDAC, voltage-dependent anion channel; HPLC, high pressure liquid chromatography.

Functional Interaction of PHGPx with SMCP

accounting for both protein thiol oxidation and selenoperoxidase moonlighting as a structural protein, was proposed as the mechanism of oxidative MC stabilization during spermatogenesis (12, 13, 15).

Although *PHGPx*^{-/-} mice are lethal and could not be analyzed for fertility (16), some insight about physiological role of PHGPx has been obtained from silencing of the nuclear form of PHGPx, which contains and N-terminal nuclear addressing sequence, produced by an alternative transcription mechanism (17). This model showed a higher sperm -SH content and transient head instability in the caudal and caput portion of the epididymis, respectively, thus proving PHGPx protein thiol peroxidase activity and structural role (18).

In situ hybridization in rat testis showed maximal PHGPx expression in the round spermatid layer (19). SMCP is also expressed in human and mouse haploid spermatid cells (9). Furthermore, in mouse spermatozoa, a subcellular co-localization of PHGPx and SMCP in the mid-piece was demonstrated by immunohistochemistry (20).

Although the specific function of the capsule remains unclear, a "protective" role seems realistic. Accordingly, silencing the gene coding for SMCP leads to infertility and asthenozoospermia in mice, although the phenotype is genetically background-sensitive and is observed only in some strains (21). In *Drosophila*, the deletion of a gene homologue of SMCP produces malformations of the axoneme and a drastic reduction in sperm motility (22). Similar defects in the assembly of mid-piece and tail have been observed in mice where the expression of selenoprotein P, which delivers selenium to cells, was abolished (23).

The co-localization of SMCP and PHGPx and the cysteine-rich nature of SMCP suggest a functional relationship, but in a previous proteomic approach, SMCP was not detected in MC (12). Therefore, by using different approaches, we decided to re-investigate the MC preparation and to clarify further the role of different proteins in the formation of the cross-linked network.

EXPERIMENTAL PROCEDURES

Preparation of Rat Spermatozoa MC—Rat spermatozoa, obtained by squeezing the cauda epididymis and the vas deferens into phosphate-buffered saline, were centrifuged at $1,500 \times g$ for 10 min and washed twice in phosphate-buffered saline. Sperm MC were prepared from spermatozoa as described by Calvin *et al.* (6), with minor modifications.

Preparation of Reduced-solubilized Capsule Proteins (RSCP)—The MCs were dissolved in 0.1 M Tris-HCl, pH 7.5, containing 0.5 $\mu\text{g/ml}$ pepstatin A, 0.7 $\mu\text{g/ml}$ leupeptin hemisulfate, 6 M guanidine-HCl, and 0.1 M 2-mercaptoethanol. Before use, small molecular weight reagents were eliminated by gel permeation chromatography repeated twice, on NAP-5 columns (Amersham Biosciences), and equilibrated with 0.01 M Tris-HCl, pH 7.6, containing 150 mM NaCl, 0.1% Triton X-100, and 1 mM EDTA. The sample was concentrated using an ultrafiltration cell equipped with a cut-off membrane of 10 kDa (Amicon Inc., Beverly, MA).

SDS-PAGE—An MC preparation was thoroughly dissolved in Laemmli sample buffer at a concentration of 4 mg/ml, and 0.1 mg was loaded on each lane of an SDS-polyacrylamide gel (T = 14%). At the end of the run, the gel was stained in colloidal Coomassie Blue, and bands were cut and digested as reported below.

In Vitro Polymerization—To 50 μg of RSCP, prepared as above, 50 μM hydrogen peroxide was added for 3 min, a time carefully calibrated in order to prevent formation of aggregates too large to be analyzed by two-dimensional redox electrophoresis. The reaction was stopped by adding sodium deoxycholate and trichloroacetic acid (0.012 and 6% (w/v), respectively). Proteins were precipitated at $4,500 \times g$ for 15 min and washed with cold ethanol.

Two-dimensional Redox Electrophoresis—The protein pellet obtained from RSCP was solubilized in 0.01 M ammonium bicarbonate, 1 mM EDTA, 1% SDS, pH 8.1, and then diluted 1:1 with Laemmli sample buffer, where 2 mM *N*-ethylmaleimide was substituted for 2-mercaptoethanol (24). Two-dimensional redox electrophoresis was performed according to Ref. 25.

Enzymatic Fragmentation, Chromatographic and Mass Spectrometric Conditions, and Data Analysis—Bands were excised from the SDS-polyacrylamide gel, digested, and analyzed as reported previously (26). The same analytical procedure was used for detecting the redox transition in synthetic peptides used as reducing substrates for the PHGPx reaction. Before injection, the assay mixture (see below) was diluted 1:10 with 0.025% trifluoroacetic acid in water.

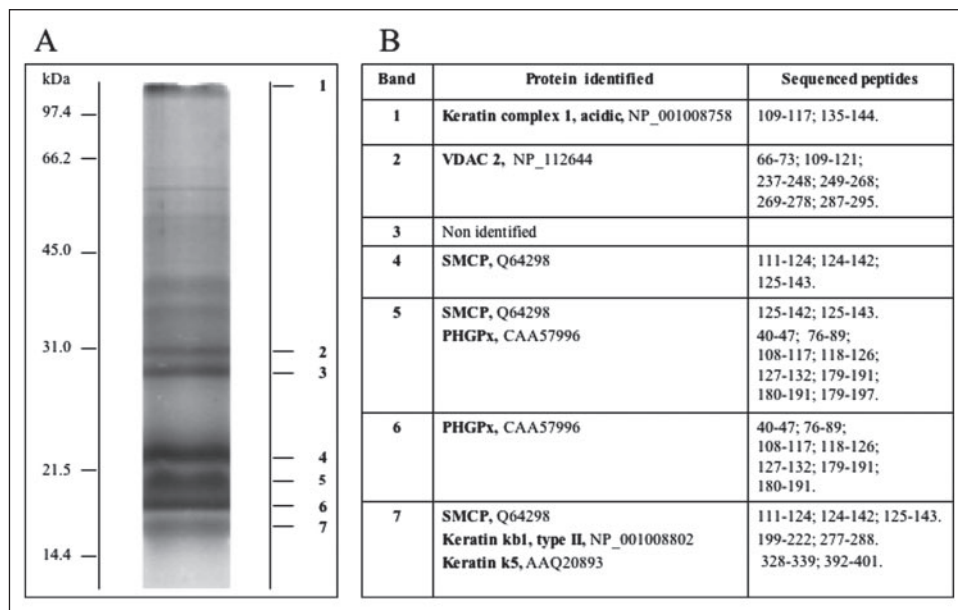
Similarity Searches—A bioinformatics approach, using sequence and domain data base searches, was employed. The proteins were extracted from the NCBI nonredundant data base (27), and the domain data bases Pfam (28), CDD (29), InterPro (30), and PROSITE (31) were searched. The sequences were searched using the BLAST, PSI-BLAST (32), HMMER (33), and ScanProsite (34) tools with default E-value cut-offs. Putative true positive hits were extracted by taking into account the adjacent cysteine repeat motif to construct a multiple alignment centered in this region using T-COFFEE (35). Proteins with a similar adjacent cysteine pattern repeat, which were annotated as hypothetical and/or lacked experimental evidence, were not considered. Manual editing was performed to keep differently spaced adjacent cysteine patterns in-frame, thus improving the alignment quality. The multiple alignment was prepared using CHROMA (www.lg.ndirect.co.uk/chroma/) (36).

Thermodynamic Calculation—A structural model of the SMCP peptide PPKPCCPQKPP was built, and its energy was minimized in different oxidation states for the Cys residues. The initial model was built by assigning the (ϕ , ψ) torsion angle combination with the highest propensity to each residue. These propensities were calculated from a data base of high resolution x-ray structures (37). Two Ala-Cys-Ala peptides were added to simulate the various disulfide-bonding patterns, which were manually imposed and minimized in various combinations. The minimization protocol consisted of 2000 conjugate gradient local minimization steps using the CHARMM package (38).

PHGPx Activity on SMCP-derived Peptides—Synthetic peptides were purchased from GenScript Corp. (www.genscript.com; Piscataway, NJ), HPLC-purified, and used as substrate for PHGPx. They were designed based on the rat/mouse SMCP sequence and contained one adjacent cysteine motif and no other cysteine residue. Before use, pig heart PHGPx (39) was treated for 30 min with 30 mM 2-mercaptoethanol on ice and then equilibrated with 0.1 M potassium phosphate, pH 7.8, containing 0.05% Triton X-100 and 1 mM EDTA, by a desalting column repeated twice (Micro Bio-Spin, Bio-Rad). The assay mixture contained 0.1 M potassium phosphate, pH 7.8, 100 μM peptide -SH groups, 1 mM EDTA, 0.8 $\mu\text{g/ml}$ PHGPx as above, in a total volume of 1 ml. Reactions were started with 50 μM H₂O₂. The thiol and H₂O₂ content were measured in 100- μl aliquots, withdrawn every 15 s. For thiol quantification, aliquots were added to 0.9 ml of 0.14 mM 5,5'-dithiobis(2-nitrobenzoic acid) dissolved in 0.05 M Tris-HCl, pH 7.9, containing 0.15 M KCl. The 5,5'-dithiobis(2-nitrobenzoic acid)-reactive material was quantified spectrophotometrically at 412 nm ($\epsilon = 13.6 \text{ cm}^{-1} \text{ mM}^{-1}$). For H₂O₂ quantification, the scopoletin/horseradish peroxidase method was used (13). Specific activity was calculated on the initial linear phase of the reaction.

Role of Cys-Cys Flanking Residues—Five peptides were designed based on the frequency of the Cys-Cys flanking residues in each of the

FIGURE 1. **Composition of rat sperm mitochondrial capsule.** A, SDS-PAGE of rat sperm MC. B, peptides identified by sequence. Excised bands (1–7) were digested by trypsin and analyzed by HPLC-ESI-MS/MS and SEQUEST analysis of MS/MS spectra. The results are representative of four independent experiments.



corresponding positions of the rat/mouse/human SMCP sequence (see Fig. 6). The reference peptide, -PKPPCCPPKP-, contained the most frequent Cys-Cys flanking residues. In the second peptide, -PPPPCCP-PPP-, the second most frequent amino acid of rat/mouse/human SMCP replaced corresponding positions for each Lys residue. The third peptide, -KKSQCCQQKT-, was designed by substituting each Pro residue with the second most frequent residue. In this peptide, the C-terminal Cys was substituted with the third most represented, in order to avoid the bias of introducing another Cys. The effect of the sequence length on PHGPx activity was evaluated by deleting one or two N- and C-terminal residues from the reference peptide. Peptides were purchased and tested as donor substrates for PHGPx, as described above.

RESULTS

Composition of Rat Sperm MC—The SEQUEST analysis of HPLC-ESI-MS/MS data of the tryptic digest of major SDS-PAGE separated bands of sperm MC nonambiguously identified the peptides reported in Fig. 1. Bands 6, 4, and 2 contained PHGPx, SMCP, and voltage-dependent anion channel (VDAC) 2, respectively. This pattern of major bands was highly reproducible, and the presence of minor components/contaminants could only be detected by a non-gel two-dimensional proteomics approach (see below). The identification of bands containing intact PHGPx and SMCP was further corroborated by Western blotting and migration of recombinant SMCP.⁴ As known from previous experience, in the case of SMCP the molecular weight calculated from electrophoretic mobility results higher than the actual molecular size (15.1 kDa), apparently because of the nonglobular structure. The electrophoretic migration of VDAC 2 roughly corresponded to the expected molecular size. The coverage of the sequence by mass spectrometry (MS) of the tryptic fragments exceeded 70% for all the proteins except SMCP, which in this case was restricted to the C terminus (amino acids 111–143). Band number 1 at the top of the gel contained peptides of keratin complex 1, acidic. For this protein of 44 kDa, there was no correspondence between electrophoretic migration and molecular size. A lack of correspondence was also observed in the following: (i) smeared band number 5, which contained peptides of both SMCP and PHGPx;

and (ii) band number 7, which contained peptides of keratin kb1, type II (65 kDa), keratin k5 (94 kDa), and SMCP. Peptide composition of band number 3, containing sequences of the nonannotated open reading frame, did not allow the identification of any known protein.

An exhaustive treatment of MC by 2-mercaptoethanol and guanidine released a series of soluble proteins here referred to as RSCP. The SDS-PAGE pattern of this material is similar to the above pattern of intact MC. The notable differences were the absence of aggregated keratin complex 1, acidic (band number 1), heterogeneous band number 5, and a less intense band number 7, containing fragments of keratins and SMCP (not shown).

A non-gel two-dimensional HPLC-MS/MS (40) analysis was also carried out on tryptic peptides released from RSCP. The above protein composition pattern was fully confirmed by this approach, although additional fragments were also detected, indicating the presence of variable minor amounts of glycerol-3-phosphate dehydrogenase, testis fatty acid-binding protein, and carnitine *O*-palmitoyltransferase I (not shown).

Similarity between SMCP and the KAP Superfamily—A bioinformatics search against the nonredundant protein data base using SMCP of rat (GenBankTM accession number Q64298), mouse (GenBankTM accession number P15265), and human (GenBankTM accession number P49901) as queries, by disabling the low complexity filters in a simple BLAST search, yielded a consistent amount of hits. These hits showed a peculiar conservation of regularly spaced adjacent cysteine patterns. The observed interval among the Cys-Cys motifs ranges from 3 to 8 residues, and most of the hits came from the superfamily of KAPs, especially from ultra-high sulfur KAP4, KAP5, and KAP9 (Fig. 2). Analysis of the adjacent cysteine flanking residues in both KAP and SMCP revealed the prevalence of Pro, charged and hydrophilic residues.

Oxidative Cross-linking of PHGPx and SMCP—RSCPs are polymerized in the presence of H₂O₂, and this reaction, catalyzed by the PHGPx activity within the sample, results in aggregates of a molecular weight high enough to prevent electrophoretic analysis and separation (13). To address the issue of the intermediates of this oxidative polymerization, we planned an experiment where the presence of inter- and intra-chain disulfides was searched by two-dimensional redox electrophoresis (25) on RSCP only partially polymerized (Fig. 3). The spots on the left side of

⁴ M. Maiorino, A. Roveri, L. Benazzi, V. Bosello, P. Mauri, S. Toppo, S. C. E. Tosatto, and F. Ursini, unpublished results.

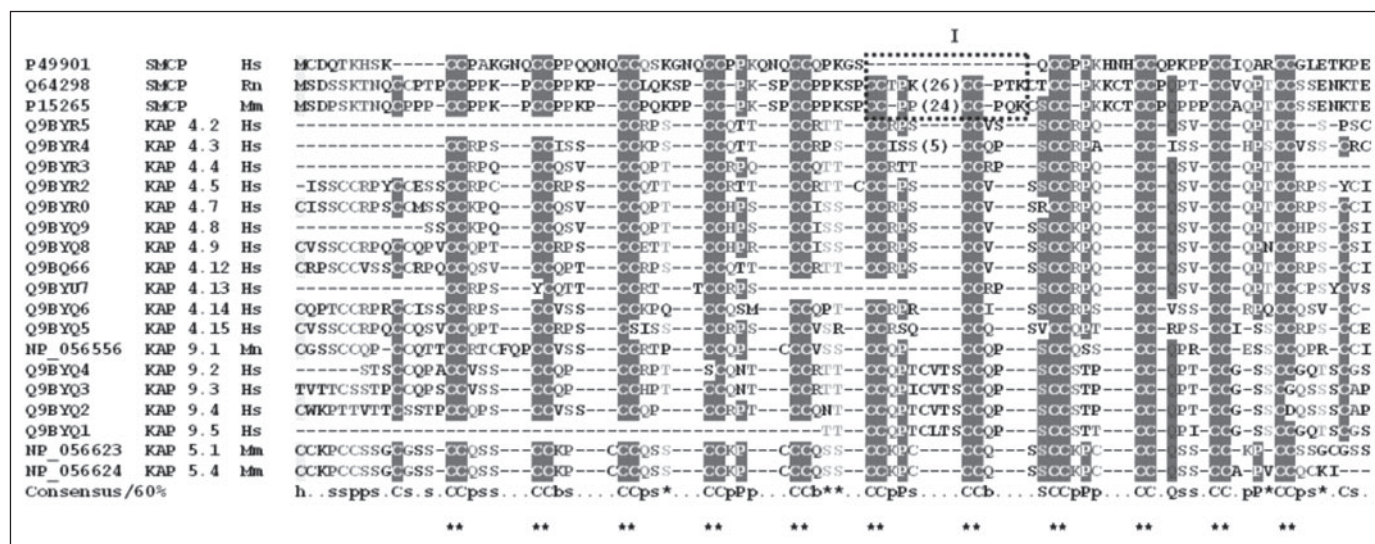


FIGURE 2. Multiple sequence alignment and a 60% consensus threshold of representative sequences from SMCP and KAPs. The final alignment was manually refined to keep the adjacent cysteine patterns highlighted with asterisks in-frame. For each protein, the accession number, a brief description, and the species are reported (*Hs*, *Homo sapiens*; *Mm*, *Mus musculus*; *Rn*, *Rattus norvegicus*). SMCP from rat and mouse have a central region of about 30 amino acids that lack the conserved Cys-Cys pattern (see box I). Only the regions of the proteins containing the repeat Cys-Cys pattern and aligning to SMCP proteins are reported. KAP proteins exhibit a conserved and repetitive pentamer containing adjacent cysteine residues, whereas SMCP proteins vary from the octamer of the human to the hexamer and heptamer of rat and mouse. Amino acid composition reflects a bias in charged and polar amino acids and prolines as shown in the consensus.

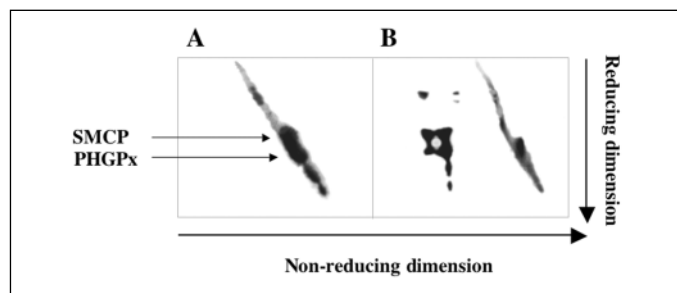


FIGURE 3. Formation of disulfides among capsular proteins. Two-dimensional redox electrophoresis of RSCP before (A) and after (B) nonexhaustive polymerization. The first and the second dimensions were run under nonreducing and reducing conditions, respectively, and were stained with Coomassie Blue. Proteins not involved in disulfide bridges have the same migration in both dimensions and remain on the diagonal of the gel. Proteins forming a homopolymer are detected as single spots on the left side of the diagonal, and proteins forming a heteropolymer are detected in a line, parallel to the second dimension. Coomassie Blue staining. PHGPx and SMCP have been identified by MS and Western blotting.

the corresponding monomeric proteins indicated the presence of polymers of PHGPx and SMCP, whereas vertically aligned spots indicated heterogeneous polymers of PHGPx, SMCP, and other proteins.

PHGPx Catalyzes the Formation of Cystine Residues from SMCP Adjacent Cysteine Motifs—The observed disulfide-dependent polymers of SMCP and PHGPx, the presence of adjacent cysteine repeats in SMCP together with the notion that disulfides between adjacent cysteine residues are prone to reshuffling (41, 42), brought to focus the hypothesis that the selenoperoxidase could be the catalyst for the formation of a cystine between SMCP adjacent cysteine residues. To verify this hypothesis, synthetic peptides from rat and mouse sequences bearing one adjacent cysteine motif were tested, as reducing substrates of PHGPx. Data reported in TABLE ONE demonstrate that adjacent cysteine residues of the different SMCP peptides are actually substrates for PHGPx, specific activity ranging from 13 to 42 μmol of thiol oxidized per min/mg of protein. Remarkably, under the same experimental conditions, the activity on peptides was higher than on glutathione for all peptides. The expected stoichiometry of 2 eq of thiol/mol of hydroperoxide was observed. Fig. 4 reports the actual time course of the reaction

TABLE ONE
PHGPx activity on adjacent cysteine residues

SMCP peptides from rat and mouse have been selected as those not presenting any Cys in the four Cys-Cys motif-flanking residues. PHGPx specific activity with glutathione, used at the peptide -SH concentration, was 13.1 $\mu\text{mol}/\text{min}/\text{mg}$ protein. Results were reproducible with a variability of less than 5%. For experimental conditions, see Fig. 4 and "Experimental Procedures."

Substrate peptide	PHGPx activity $\mu\text{mol}/\text{min}/\text{mg}$ protein
PPKCCPPKP	25.2
QKPPCCPKSP	37.5
PKSPCCPPKS	42.0
PKSPCCPPKP	13.6
QKSPCCPKSP	36.0

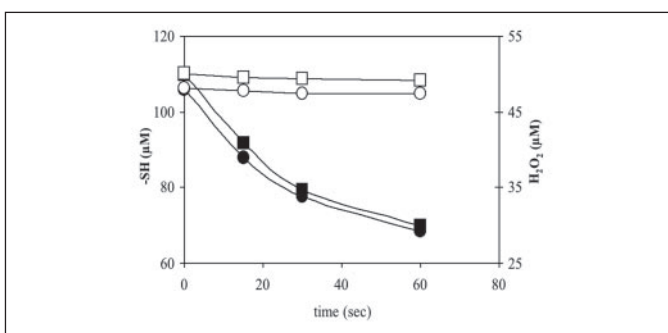


FIGURE 4. Peroxidatic reaction of PHGPx with H_2O_2 and peptide PPKCCPPKP. Reaction was started by adding 50 μM H_2O_2 and measured on aliquots withdrawn at different times for thiol (circle) and H_2O_2 (squares). Reactions were carried out in the presence of 100 μM peptide thiol and 0.8 $\mu\text{g}/\text{ml}$ of PHGPx purified from pig heart (filled circles and squares) or without any enzyme (open circles and squares). See "Experimental Procedures" for details.

for the peptide PPKCCPPKP, among the longest SMCP peptides containing one Cys-Cys doublet and no other Cys residue in the mouse sequence. In this case, as for some other peptides, the reaction did not reach completeness. This aspect, related to the final equilibrium of the reaction and the possible formation of dead-end intermediates, was not further investigated.

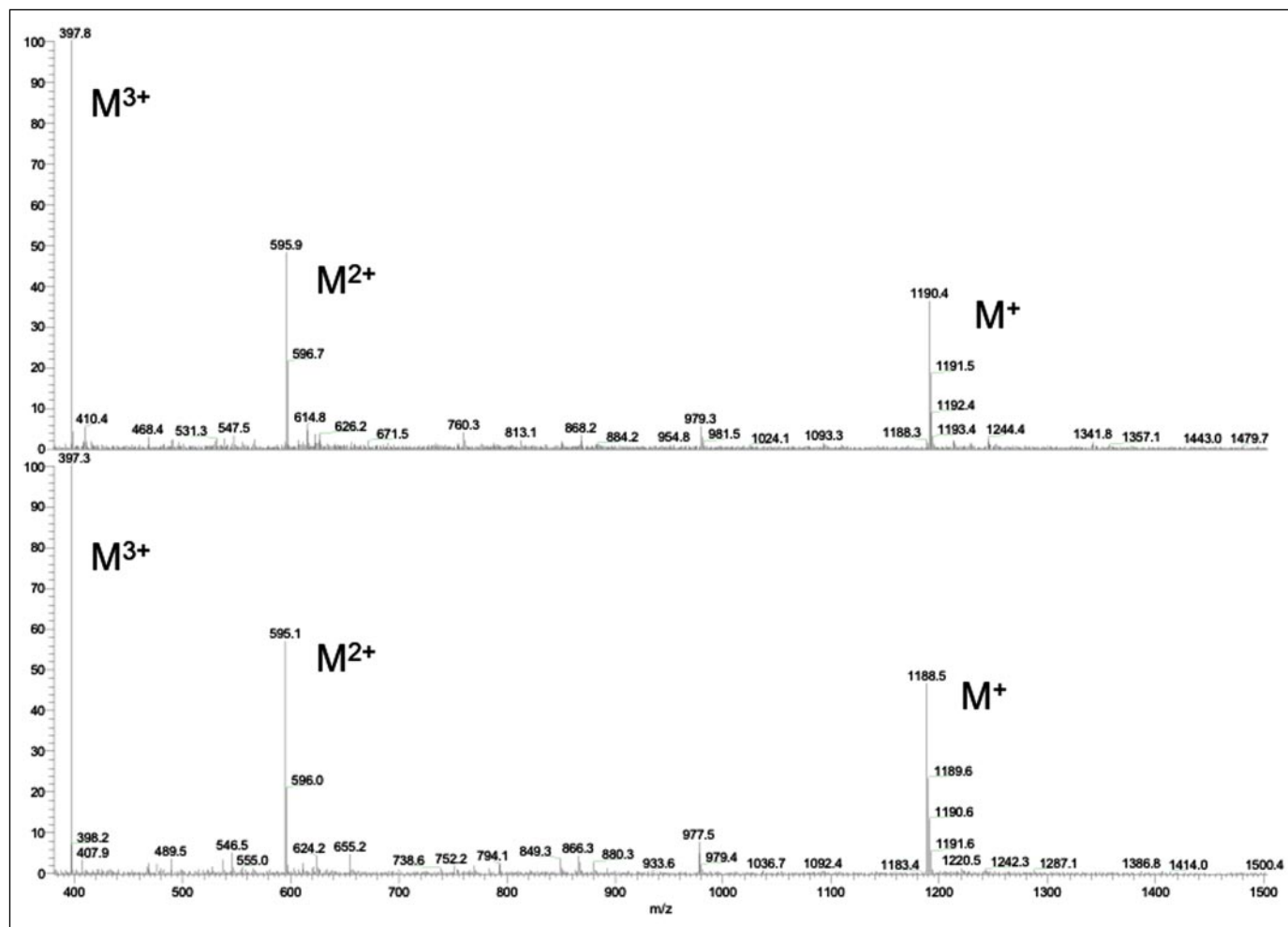


FIGURE 5. **Formation of a cystine between adjacent cysteines.** HPLC ESI-MS spectra of the peptide PPKPCCPQKPP before (upper panel) and after (lower panel) the reaction of PHGPx with H_2O_2 . Reaction was carried out under the conditions of Fig. 4. One minute after the addition of H_2O_2 , the sample was diluted 1:10 with 0.025% trifluoroacetic acid in water, and an aliquot was analyzed immediately.

Formation of the disulfide between adjacent cysteine residues was validated by MS analysis of the reaction product. The spectra of the reduced and enzymatically oxidized peptide PPKPCCPQKPP are reported as an example in Fig. 5. The difference of 2 atomic mass units between oxidized and reduced peptides supports the redox transition, and the presence of multicharged ions (M^+ , M^{2+} , and M^{3+}) rules out the possibility that the oxidized peptide is a dimer. MS/MS analysis supported this conclusion (not shown).

From the amino acid sequence flanking the adjacent Cys motif, a clear-cut consensus sequence for maximal activity was not evident. Nevertheless, because Pro and Lys residues were the most represented amino acids in the primary sequence of rat/mouse/human SMCP (Fig. 2), we tested how substitution of these two amino acids affects PHGPx activity. The results reported in TABLE TWO show that substituting Pro for Lys residues, according to the strategy reported under "Experimental Procedures" and based on the data reported in Fig. 6, increases activity. On the other hand, substituting Lys for Pro practically abolishes activity. Also deleting one N- and one C-terminal residue abolishes activity, but this is possibly not because of the length, because by deleting one additional N- and C-terminal residue, the activity was instead rather high.

Reshuffling of the Disulfide among Adjacent Cysteine Residues Is Thermodynamically Favorable—To get further support for the concept that the disulfide bond between adjacent Cys residues in SMCP is prone to

TABLE TWO

Effect of Cys-Cys flanking amino acids on PHGPx activity

Peptides were designed as reported under "Experimental Procedures" from the sequence frequency reported in Fig. 6 and contained the most represented amino acids around the Cys-Cys motif. Results were reproducible with a variability of less than 5%. For experimental conditions, see TABLE ONE.

Substrate peptide	PHGPx activity $\mu\text{mol}/\text{min}/\text{mg protein}$
PKPPCCPPKP	28.3
PPPCCPPPP	69.0
KKSQCCQKKT	0.3
KPPCCPPK	0.4
PPCCPP	160.2

reshuffling, as has been described for model proteins (41, 42), we adopted a thermodynamic approach. As expected, the energy minimization data of all possible disulfide arrangements (Fig. 7) clearly demonstrated that there is a distinct energetic disadvantage for the peptide to form adjacent disulfides and that the reshuffled conformation involving the maximum number of disulfide bonds is energetically favored. The proposal that once the adjacent disulfide is formed, it will eventually undergo a disulfide reshuffling leading to polymerization is therefore reasonable and is supported by thermodynamics.

Functional Interaction of PHGPx with SMCP

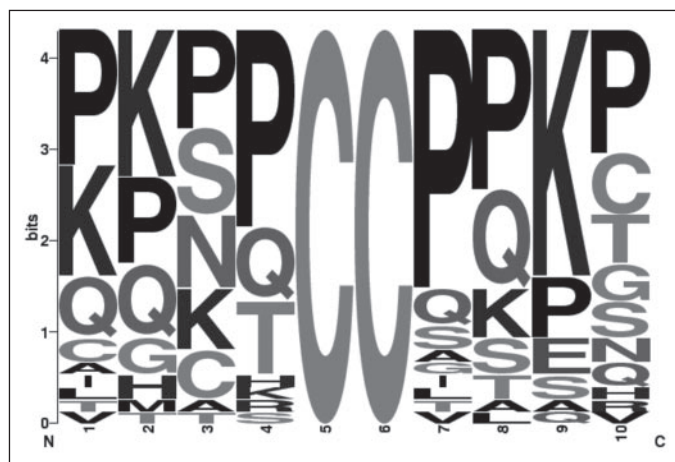


FIGURE 6. **Sequence logo of SMCP.** The representation is displayed for the repeats detected in SMCP of rat, mouse, and human containing the adjacent cysteine residues in the center. Each logo consists of stacks of amino acids for each position in the sequence. The height of symbols within the stack indicates the relative frequency of each amino acid at that position.

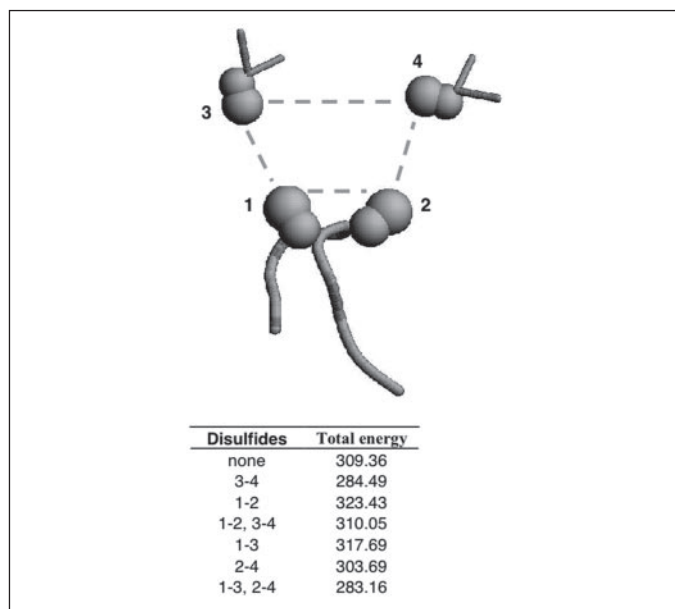


FIGURE 7. **Reshuffling of a disulfide among adjacent cysteine residues.** Schematic representation of the SMCP peptide PPKPCCPQKPP and two proximal Ala-Cys-Ala peptides used to simulate the different disulfide bonding patterns. The β -carbon and γ -sulfur atoms are shown as spheres and bonding patterns are highlighted by dashed lines. The combinations between the four cysteine residues and their associated energies (in kcal/mol) are reported.

DISCUSSION

The major proteins of rat MC are PHGPx, SMCP, VDAC 2, and some members of the keratin family. The positive identification of SMCP and keratins we obtained by ESI-MS/MS expands the previous information obtained by two-dimensional gel and matrix-assisted laser desorption ionization time-of-flight analysis (12). Apparently, in the previous study, loss of these proteins took place during solubilization and focusing. We indeed observed that keratins are lost when RSCP is solubilized as in Ref. 12, and SMCP does not focalize in isoelectrofocusing gels.

SMCP was detected both by SDS-PAGE of MC (Fig. 1) and RSCP and by a non-gel two-dimensional MS approach on RSCP. The identification was nonambiguous, although only the C terminus of the protein was positively identified by the SEQUEST analysis of MS/MS data, apparently because of the large number of trypsin cleavage sites in the

rat SMCP primary sequence, thus giving rise to fragments too small to be analyzed accurately.

In light of the most recent data, the presence of VDAC 2 in MC is not surprising. It has been reported that VDACs may have a cytoskeletal localization, and more specifically, in bovine sperm cells VDAC 2 and 3 are linked to the outer dense fibers, a cytoskeletal component of sperm flagellum, and VDAC 2 to mitochondria (43). The present data highlight the association of VDAC with MC as a cytoskeleton-related structure.

Of the keratins identified, keratin complex 1, acidic, and keratin kb1 belong to the class of cysteine-rich cytokeratins, whereas keratin k5 contains only some cysteine residues.

Acidic keratin complex 1 was detected in an aggregated form from which the single chain is not released under SDS-PAGE conditions. Fragments of type II keratin kb1 and keratin k5 were detected instead in a single band at a molecular weight lower than expected and containing fragments of SMCP (Fig. 1, band 7). At first glance, this could be attributed to the proteolytic step of the MC preparation. Moreover, this was not the only heterogeneous band where SDS-PAGE migration was in marked disagreement with the expected molecular weight. Fragments of both SMCP and PHGPx were detected in smeared band 5, although the migration was faster than SMCP and slower than PHGPx. A reasonable interpretation of these intriguing results is that peptides in band 5 are released from a large complex containing both PHGPx and SMCP. The complex is most likely partially digested by trypsin during the MC preparation and is resistant to reduction. The notion of the presence of a heterogeneous protein complex cross-linked and partially digested could also apply to the low molecular weight band 7, containing SMCP and proteins of the keratin family. A cross-linking made up by bonds other than disulfides, such as transglutaminase-mediated covalent isopeptide protein-protein cross-links, could account for this evidence, but this hypothesis was not further investigated.

The conclusion that smeared bands 5 and 7 are produced from larger aggregates by trypsin treatment during MC preparation was further supported by the observation that these bands are not present when MCs are prepared in the absence of trypsin.³ Unfortunately, this preparation was not suitable for further studies because it also resulted in heavily contaminated vesicles morphologically different from MC and containing components of the sperm tail principal piece such as AKAP 4 (GenBankTM accession number NP_077378), AKAP3 (GenBankTM accession number Q66HC6), and GST M5 (GenBankTM accession number Q9Z1B2).

The identification of proteins of the keratin family in MC would not appear to be particularly impressive, because the structure is actually referred to as "keratinous." On the other hand, specific proteins have not been identified previously. Their presence is particularly appealing in the light of the observation that SMCP can be viewed as a KAP. A common sequence motif was detected in SMCP and the class of ultra-high sulfur KAPs, which builds upon the regularly spaced repetition of adjacent cysteine residues (Fig. 2).

KAPs were first identified as a major component of the hair fiber matrix, involved in the formation of the rigid hair shaft by cross-linking keratin intermediate filaments to form a complex meshwork (44, 45). Members from the KAP families bundle keratin intermediate filaments by a complex system of disulfide bonds conferring rigidity (45).

The different spacing of the adjacent cysteine pattern found in KAPs and SMCP does not seem to affect the functional link. A certain variation of spacing is indeed already present among SMCP proteins from different species, suggesting that a key role is played by the repeats of adjacent cysteine residues regularly spaced in the same protein, whereas the distance among the repeats does not result in a major constraint.

MC proteins reduced and solubilized (RSCP) undergo oxidative polymerization in the presence of H₂O₂ leading to large aggregates where practically all the capsule proteins are embedded, and where the indispensable catalyst is PHGPx (12, 13).

Here we present evidence for the central role of SMCP, as a PHGPx substrate, in this oxidative polymerization (Fig. 3). The PHGPx-catalyzed oxidation of SMCP cysteine residues results in both homo- and heteropolymerization through the peroxidic mechanism and formation of dead-end seleno-disulfide intermediates described for the homopolymerization of PHGPx (14).

The specific involvement of the Cys-Cys doublet of SMCP, as substrate of the reaction of PHGPx, suggested by the above evidence, was specifically tested on synthetic SMCP-derived peptides (TABLE ONE) and resulted in the disclosure of a new unexpected activity of PHGPx. All tested SMCP peptides are good reducing substrates for PHGPx reaction with the expected 2:1 thiol/peroxide stoichiometry (Fig. 4). The reaction produces a cystine between adjacent cysteine residues, as nonambiguously demonstrated by MS analysis of the reaction product (Fig. 5). To our knowledge, this is the first report showing that an enzyme is involved in the oxidation of adjacent cysteine residues. The PHGPx activity on peptides is higher than on glutathione. Although unexpected, this result is not fully surprising when considering that PHGPx prefers synthetic substrates containing two thiol groups (46). The only relevant structural constraint we succeeded in identifying for this reaction is the requirement for Pro residues (TABLE TWO). The Lys residues, quite often present in the positions flanking the Cys-Cys doublet (Fig. 6), negatively affect the activity, thus suggesting a function different from the protein-peptide interaction. Therefore, the sole requirement we can deduce so far is the peculiar rigidity of the backbone of the peptide brought about by the polyprolyl structure.

The formation of a disulfide among adjacent cysteine motifs generates an unusual eight-membered ring imposing a specific angle to the protein backbone, described as a conformational redox switch (41, 42). In addition, this unusual disulfide is highly prone to reshuffling and has been shown to be an intermediate in directing the protein folding that leads to the formation of a peculiar knotting fold (42). This supports our proposal that the cystine residue produced by PHGPx on SMCP Cys-Cys motifs is very likely only the transient intermediate of polymerization. The reshuffling of SMCP cystine residues, leading to the assembly and stabilization of spermatozoa MC, is indeed supported by the thermodynamic calculation of energetic gain brought about by the process (Fig. 7), although the positive direct demonstration of the thiol-disulfide exchange is still lacking. Occurrence of a reshuffling is also consistent with our unpublished observations³ that oxidation of recombinant SMCP in the presence of PHGPx produces an extremely complex array of disulfides, among which those between the adjacent cysteine residues were not detected.

The participation of keratins in the formation of MC endorses the KAP nature of SMCP; SMCP is oxidized by PHGPx, and this primes the interaction with keratins and other proteins in forming the MC. Although we have only indirect evidence for the presence of disulfides linking SMCP and keratins, *i.e.* the reductive solubilization of MC yielding RSCP, the similarity with the process where KAPs cross-link hair cytokeratins during hair formation is stimulating.

In conclusion, from this evidence and in complete agreement with PHGPx enzymology, we propose that the selenium catalysis on SMCP produces a kind of "biochemical glue" holding together sperm tail keratins and functional structures. Moreover, polymerization, as directly obtained by the reaction of PHGPx on SMCP, is possibly not the actual final structure. An editing of the disulfide pattern in oxidized sperm

structures has been suggested recently to take place via thioredoxin and a testis-specific glutathione-thioredoxin reductase (47), although neither of these proteins has been detected among MC proteins.

A defective function of the process gives a reasonable account for the structural defects observed both during selenium deficiency in the rat (2, 48–50) and following deletion of the selenoprotein P, which is involved in selenium supply to tissues (23).

The wide tissue distribution of PHGPx might suggest that the above mechanism is not solely restricted to spermatogenesis but may take place in other tissues and for other functions where different keratins and different KAPs are involved. Because glutathione competes with adjacent cysteine residues as a reducing substrate for PHGPx, the cellular redox status emerges as the priming agent for such a mechanism of functional redox switch.

REFERENCES

- Brown, D. G., and Burk, R. F. (1973) *J. Nutr.* **103**, 102–108
- Wu, S. H., Oldfield, J. E., Whanger, P. D., and Weswig, P. H. (1973) *Biol. Reprod.* **8**, 625–629
- Calvin, H. I. (1978) *J. Exp. Zool.* **204**, 445–452
- Pallini, V., and Bacci, E. (1979) *J. Submicrosc. Cytol.* **11**, 165–170
- Calvin, H. I., and Cooper, G. W. (1979) in *The Spermatozoon* (Fawcett, D. W., and Bedford, J. M., eds) pp. 135–140, Urban & Schwarzenberg, Inc., Baltimore
- Calvin, H. I., Cooper, G. W., and Wallace, E. (1981) *Gamete Res.* **4**, 139–149
- Karimpour, I., Cutler, M., Shih, D., Smith, J., and Kleene, K. C. (1992) *DNA Cell Biol.* **11**, 693–699
- Chambers, I., Frampton, J., Goldfarb, P., Affara, N., McBain, W., and Harrison, P. R. (1986) *EMBO J.* **5**, 1221–1227
- Aho, H., Schwemmer, M., Tessman, D., Murphy, D., Mattei, G., Engel, W., and Adham, I. M. (1996) *Genomics* **32**, 184–190
- Cataldo, L., Baig, K., Oko, R., Mastrangelo, M. A., and Kleene, K. C. (1996) *Mol. Reprod. Dev.* **45**, 320–331
- Adham, I. M., Tessmann, D., Soliman, K. A., Murphy, D., Kremling, H., Szpirer, C., and Engel, W. (1996) *DNA Cell Biol.* **15**, 159–166
- Ursini, F., Heim, S., Kiess, M., Maiorino, M., Roveri, A., Wissing, J., and Flohé, L. (1999) *Science* **285**, 1393–1396
- Roveri, A., Ursini, F., Flohé, L., and Maiorino, M. (2001) *Biofactors* **14**, 213–222
- Mauri, P., Benazzi, L., Flohé, L., Maiorino, M., Pietta, P. G., Pilawa, S., Roveri, A., and Ursini, F. (2003) *Biol. Chem.* **384**, 575–588
- Maiorino, M., and Ursini, F. (2002) *Biol. Chem.* **383**, 591–597
- Imai, H., Hirao, F., Sakamoto, T., Sekine, K., Mizukura, Y., Saito, M., Kitamoto, T., Hayasaka, M., Hanaoka, K., and Nakagawa, Y. (2003) *Biochem. Biophys. Res. Commun.* **305**, 278–286
- Maiorino, M., Scapin, M., Ursini, F., Biasolo, M., Bosello, V., and Flohé, L. (2003) *J. Biol. Chem.* **278**, 34286–34290
- Conrad, M., Moreno, S. G., Sinowatz, F., Ursini, F., Kolle, S., Roveri, A., Brielmeier, M., Wurst, W., Maiorino, M., and Bornkamm, G. W. (2005) *Mol. Cell. Biol.* **25**, 7637–7644
- Maiorino, M., Wissing, J. B., Brigelius-Flohé, R., Calabrese, F., Roveri, A., Steinert, P., Ursini, F., and Flohé, L. (1998) *FASEB J.* **12**, 1359–1370
- Nayernia, K., Diaconu, M., Aumuller, G., Wennemuth, G., Schwandt, I., Kleene, K., Kuehn, H., and Engel, W. (2004) *Mol. Reprod. Dev.* **67**, 458–464
- Nayernia, K., Adham, I. M., Burkhardt-Gottges, E., Neesen, J., Rieche, M., Wolf, S., Sancken, U., Kleene, K., and Engel, W. (2002) *Mol. Cell. Biol.* **22**, 3046–3052
- Kuhn, R., Kuhn, C., Borsch, D., Glatzer, K. H., Schafer, U., and Schafer, M. (1991) *Mech. Dev.* **35**, 143–151
- Olson, G. E., Winfrey, V. P., Nagdas, S. K., Hill, K. E., and Burk, R. F. (2005) *Biol. Reprod.* **73**, 201–211
- Laemmli, U. K. (1970) *Nature* **227**, 680–685
- Traut, R. R., Casiano, C., and Zecherle, N. (1989) in *Protein Function: A Practical Approach* (Creighton, T. E., ed) pp. 101–133, IRL Press at Oxford University Press, Oxford
- Maiorino, M., Mauri, P., Roveri, A., Benazzi, L., Toppo, S., Bosello, V., and Ursini, F. (2005) *FEBS Lett.* **579**, 667–670
- Pruitt, K. D., Tatusova, T., and Maglott, D. R. (2003) *Nucleic Acids Res.* **31**, 34–37
- Bateman, A., Coin, L., Durbin, R., Finn, R. D., Hollich, V., Griffiths-Jones, S., Khanna, A., Marshall, M., Moxon, S., Sonnhammer, E. L., Studholme, D. J., Yeats, C., and Eddy, S. R. (2004) *Nucleic Acids Res.* **32**, D138–D141
- Marchler-Bauer, A., Anderson, J. B., DeWeese-Scott, C., Fedorova, N. D., Geer, L. Y., He, S., Hurwitz, D. I., Jackson, J. D., Jacobs, A. R., Lanczycki, C. J., Liebert, C. A., Liu, C., Madej, T., Marchler, G. H., Mazumder, R., Nikolskaya, A. N., Panchenko, A. R., Rao, B. S., Shoemaker, B. A., Simonyan, V., Song, J. S., Thiessen, P. A., Vasudevan, S.,

Functional Interaction of PHGPx with SMCP

- Wang, Y., Yamashita, R. A., Yin, J. J., and Bryant, S. H. (2003) *Nucleic Acids Res.* **31**, 383–387
30. Mulder, N. J., Apweiler, R., Attwood, T. K., Bairoch, A., Barrell, D., Bateman, A., Binns, D., Biswas, M., Bradley, P., Bork, P., Bucher, P., Copley, R. R., Courcelle, E., Das, U., Durbin, R., Falquet, L., Fleischmann, W., Griffiths-Jones, S., Haft, D., Harte, N., Hulo, N., Kahn, D., Kanapin, A., Krestyaninova, M., Lopez, R., Letunic, I., Lonsdale, D., Silventoinen, V., Orchard, S. E., Pagni, M., Peyruc, D., Ponting, C. P., Selengut, J. D., Servant, F., Sigrist, C. J., Vaughan, R., and Zdobnov, E. M. (2003) *Nucleic Acids Res.* **31**, 315–318
31. Hulo, N., Sigrist, C. J., Le Saux, V., Langendijk-Genevaux, P. S., Bordoli, L., Gattiker, A., De Castro, E., Bucher, P., and Bairoch, A. (2004) *Nucleic Acids Res.* **32**, D134–D137
32. Altschul, S. F., Madden, T. L., Schaffer, A. A., Zhang, J., Zhang, Z., Miller, W., and Lipman, D. J. (1997) *Nucleic Acids Res.* **25**, 3389–3402
33. Eddy, S. R. (1996) *Curr. Opin. Struct. Biol.* **6**, 361–365
34. Gattiker, A., Gasteiger, E., and Bairoch, A. (2002) *Appl. Bioinformatics* **1**, 107–108
35. Notredame, C., Higgins, D. G., and Heringa, J. (2000) *J. Mol. Biol.* **302**, 205–217
36. Goodstadt, L., and Ponting, C. P. (2001) *Bioinformatics* **17**, 845–846
37. Lovell, S. C., Davis, I. W., Arendall, W. B. R., de Bakker, P. I., Word, J. M., Prisant, M. G., Richardson, J. S., and Richardson, D. C. (2003) *Proteins* **50**, 437–450
38. MacKerell, J. A. D., Bashford, D., Bellott, M., Dunbrack, R. L., Evanseck, J., Field, M. J., Fischer, S., Gao, J., Guo, H., Ha, S., Joseph-McCarthy, D., Kuchnir, L., Kuczera, K., Lau, F. T. K., Mattos, C., Michnick, S., Ngo, T., Nguyen, D. T., Prodhom, B., Reiher, W. E., Roux, B., Schlenkrich, M., Smith, J. C., Stote, R., Straub, J., Watanabe, M., Wiorkiewicz-Kuczera, J., Yin, D., and Karplus, M. (1998) *J. Phys. Chem. B* **102**, 3586–3616
39. Maiorino, M., Gregolin, C., and Ursini, F. (1990) *Methods Enzymol.* **186**, 448–457
40. Mauri, P. L., Scarpa, A., Nascimbeni, A. C., Benazzi, L., Parmagnani, E., Mafficini, A., Della Peruta, M., Bassi, C., Miyazaki, K., and Sorio, C. (2005) *FASEB J.* **19**, 1125–1127
41. Park, C., and Raines, R. T. (2001) *Protein Eng.* **14**, 939–942
42. Cemazar, M., Zahariev, S., Lopez, J. J., Carugo, O., Jones, J. A., Hore, P. J., and Pongor, S. (2003) *Proc. Natl. Acad. Sci. U. S. A.* **100**, 5754–5759
43. Hinsch, K. D., De Pinto, V., Aires, V. A., Schneider, X., Messina, A., and Hinsch, E. (2004) *J. Biol. Chem.* **279**, 15281–15288
44. Powell, B. C., and Rogers, G. E. (1997) *Exs (Basel)* **78**, 59–148
45. Rogers, M. A., Langbein, L., Winter, H., Beckmann, I., Praetzel, S., and Schweizer, J. (2004) *J. Invest. Dermatol.* **122**, 147–158
46. Roveri, A., Maiorino, M., Nisii, C., and Ursini, F. (1994) *Biochim. Biophys. Acta* **1208**, 211–221
47. Su, D., Novoselov, S. V., Sun, Q. A., Moustafa, M. E., Zhou, Y., Oko, R., Hatfield, D. L., and Gladyshev, V. N. (2005) *J. Biol. Chem.* **280**, 26491–26498
48. Wallace, E., Cooper, G. W., and Calvin, H. I. (1983) *Gamete Res.* **4**, 389–399
49. Wallace, E., Calvin, H. I., and Cooper, G. W. (1983) *Gamete Res.* **4**, 377–387
50. Wu, S. H., Oldfield, J. E., Shull, L. R., and Cheeke, P. R. (1979) *Biol. Reprod.* **20**, 793–798